





Interactions between host epithelial cells and *Acinetobacter baumannii* promote the emergence of highly antibiotic resistant and highly mucoid strains

Wang Zhang ^{a,b,c,*}, Yue Yao ^{a,b,c,*}, Hua Zhou ^{d*}, Jintao He ^{a,b,c}, Jingfen Wang ^{a,b,c}, Li Li^e, Minsong Gao^f, Xiaochen Liu ^{a,b,c}, Ya Shi^g, Jinzhong Lin^e, Jianzhao Liu^{f,h}, Huan Chen^g, Yu Feng^{a,i}, Zhihui Zhou ^{a,b,c}, Yunsong Yu ^{a,b,c} and Xiaoting Hua ^{a,b,c}

^aDepartment of Infectious Diseases, Sir Run Run Shaw Hospital, Zhejiang University School of Medicine, Hangzhou, People's Republic of China; ^bRegional Medical Center for National Institute of Respiratory Diseases, Sir Run Run Shaw Hospital, Zhejiang University School of Medicine, Hangzhou, People's Republic of China; ^cKey Laboratory of Microbial Technology and Bioinformatics of Zhejiang Province, Hangzhou, People's Republic of China; ^dDepartment of Respiratory and Critical Care Medicine, The First Affiliated Hospital, Zhejiang University School of Medicine, Hangzhou, People's Republic of China; ^eState Key Laboratory of Genetic Engineering, School of Life Sciences, Zhongshan Hospital, Fudan University, Shanghai, People's Republic of China; ^fMOE Key Laboratory of Macromolecular Synthesis and Functionalization, Department of Polymer Science and Engineering, Zhejiang University, Hangzhou, People's Republic of China; ^gHangzhou Digital-Micro Biotech Co., Ltd., Hangzhou, People's Republic of China; ^hLife Sciences Institute, Zhejiang University, Hangzhou, People's Republic of China; ⁱDepartment of Biophysics, Zhejiang University School of Medicine, Hangzhou, People's Republic of China

ABSTRACT

Acinetobacter baumannii is an important nosocomial pathogen. Upon colonizing a host, *A. baumannii* are subjected to selective pressure by immune defenses as they adapt to the host environment. However, the mechanism of this pathoadaptation is unknown. Here, we established an *in vitro* system to evolve *A. baumannii* driven by the continuous selective pressure exerted by epithelial cells, and we used a combination of experimental evolution, phenotypic characterization and multi-omics analysis to address the underlying mechanism. When continuously exposed to selective pressure by pulmonary epithelial cells, *A. baumannii* showed *ptk* mutation-mediated mucoid conversion (reduced adhesion and increased anti-phagocytic ability) by enhancement of capsular exopolysaccharide chain length; *rsmG* mutation-mediated deficiency of 7-methylguanosine modification in the 524th nucleotide of 16S rRNA, which increased ribosome translation efficiency; and *rnaseI* mutation-mediated changes in outer membrane permeability and efflux pump expression. Together, these mutations altered susceptibility to a variety of antimicrobial agents, including the novel antibiotic cefiderocol, by regulating siderophore and siderophore-receptor biosynthesis. In conclusion, pulmonary epithelial cells modulate *A. baumannii* pathoadaptation, implicating the host-microbe interaction in the survival and persistence of *A. baumannii*.

ARTICLE HISTORY Received 1 June 2022; Revised 8 October 2022; Accepted 11 October 2022





KEYWORDS *Acinetobacter baumannii*; pathoadaptation; epithelial cell; experimental evolution; antibiotic resistance; mucoid phenotype

Introduction


Upon colonizing a host, bacterial pathogens rapidly adapt to survive under multiple selective pressures. Invading bacteria must overcome host defenses, including nutrient limitation and immune response [1]. Bacterial pathogens have evolved numerous strategies to this end [2], for example, by acquiring new gene by horizontal gene transfer or by undergoing pathoadaptive mutations [3]. Pathogen mutations during persistent host infection are likely to be pathoadaptive [4,5].

Acinetobacter baumannii, an opportunistic pathogen, is increasing in incidence, and is prevalent in hospital environments, particularly in intensive care units

and in patients with pneumonia and bacteremia [6]. Translocation of *A. baumannii* from the lungs to the bloodstream is associated with severe complications (e.g. sepsis), particularly in immunosuppressed patients or those on mechanical ventilation, leading to a high mortality rate [7]. Virulence factors such as *OmpA*, lipopolysaccharides, and capsule [8,9] mediate host colonization and damage. Especially, capsular exopolysaccharide and associated mucoid phenotype have emerged as a universal virulence factor owing to several observations [10]. Previous evidence supports a role for capsule structures in contributing to defenses against antibiotics such as antimicrobial peptides [11–13]. Because of the variability of the

CONTACT Yunsong Yu  yvys119@zju.edu.cn  Department of Infectious Diseases, Sir Run Run Shaw Hospital, Zhejiang University School of Medicine, 3 East Qingchun Road, Hangzhou, Zhejiang, 310016, People's Republic of China; Xiaoting Hua  xiaotinghua@zju.edu.cn  Department of Infectious Diseases, Sir Run Run Shaw Hospital, Zhejiang University School of Medicine, 3 East Qingchun Road, Hangzhou, Zhejiang, 310016, People's Republic of China

*These authors contributed equally to this work.

 Supplemental data for this article can be accessed online at <https://doi.org/10.1080/22221751.2022.2136534>.

© 2022 The Author(s). Published by Informa UK Limited, trading as Taylor & Francis Group, on behalf of Shanghai Shangyixun Cultural Communication Co., Ltd
This is an Open Access article distributed under the terms of the Creative Commons Attribution-NonCommercial License (<http://creativecommons.org/licenses/by-nc/4.0/>), which permits unrestricted non-commercial use, distribution, and reproduction in any medium, provided the original work is properly cited.

Acinetobacter genome, adaptive evolution under host stress can also promote persistence [14].

The lung is the main colonization and infection site of *A. baumannii*, and the airway epithelium is the first line of defense against invasion by pathogenic microorganisms [15,16]. Epithelial cells trigger the host inflammatory response [17]. Although epithelial cells are nonspecific phagocytes, they are important in the pathogenesis of *A. baumannii* [18]. *A. baumannii* changes at multiple levels as it interacts with a host, for example, undergoing transcriptome remodelling and gene mutation [19–21]. Experimental evolution in controlled environments that mimic host selective pressures, combined with advanced DNA sequencing techniques, enables the investigation of adaptive evolution. To the best of our knowledge, the host cell-mediated adaptive evolution of *A. baumannii* has not been investigated using an experimental evolution model.

We established an *in vitro* system to evolve *A. baumannii* under continuous selective pressure from epithelial cells. Epithelial cell-adapted clones displayed not only the ability to evade adherence and phagocytosis due to a mucoid phenotype but also increased resistance to several antibiotics.

Materials and methods

Bacterial strains, cells, plasmids, and infection procedure

The wild-type (WT) *A. baumannii* strain ATCC17978 was used, and ASD9 and ACD9 were obtained from a laboratory evolution experiment (Table S1). One-step chromosomal gene mutation based on recombination-mediated genetic engineering (pMo130-Hyg) was performed to establish mutant strains; the pYMAb2-Hyg shuttle vector was used to establish gene-complemented strains (Table S1). Strains were cultured in Mueller-Hinton (MH) Broth (Oxoid; Thermo Scientific, Waltham, MA); gene-complemented strains were cultured in MH Broth supplemented with hygromycin (100 µg/mL). All strains were grown at 37°C.

The A549 human pulmonary adenocarcinoma cell line (#CCL185; ATCC, Manassas, VA) and HBE human bronchial epithelial cell line (#CRL2741; ATCC, Manassas, VA) were cultivated in Dulbecco's modified Eagle's medium (Cat. No: 10-013-CV; Corning Inc., Corning, NY) supplemented with 10% fetal bovine serum (35-081-CV; Corning Inc., Corning, NY) and 1% penicillin/streptomycin (Cat. No: 30-002-CI; Corning Inc., Corning, NY) and incubated at 37°C in an atmosphere of 5% CO₂. THP-1 human monocytes were cultivated in Roswell Park Memorial Institute-1640 medium (10-040-CV; Corning Inc., Corning, NY) with 10% fetal bovine serum and 1% penicillin/streptomycin. THP-1 cells were differentiated into macrophage-like cells (THP-1 Mø) by incubation in

the presence of phorbol myristate acetate (Cat. No: HY-18739; MCE, Monmouth Junction, NJ) at 200 ng/mL for 48 h. For cell infection, fetal bovine serum-free medium without penicillin/streptomycin containing bacteria at a multiplicity of infection (MOI) of 100 was added to cell plates and incubated at 37°C in a 5% CO₂ atmosphere.

Laboratory evolution experiment

A single colony of ATCC17978 was cultured in 2 mL MH broth overnight at 37°C. Fetal bovine serum-free medium without penicillin/streptomycin containing bacteria at an MOI of 1:1 (10⁶ *A. baumannii* to 10⁶ cells) was added to cell flasks and incubated for 24 h at 37°C in an atmosphere of 5% CO₂, which was considered a passage. Bacteria were subsequently bottlenecked to start the next passage. As a control, equal numbers of bacteria evolved under identical conditions in the absence of cells. All populations evolved for 9 days, and populations on days 3, 6, and 9 were collected. The populations that evolved with and without cells were designated A1/A2/A3 and H1/H2/H3, and A4/A5/A6 and H4/H5/H6, respectively.

Genomic DNA sequencing and analysis

The genomic DNA of ACD9 and HCD9 was extracted using a QIAamp DNA Minikit (Qiagen Valencia, CA) following the manufacturer's protocol. Libraries were prepared using the TruePrep™ DNA Library Prep Kit V2 for Illumina (Vazyme, Nanjing, China). Using a single “transposase” enzymatic reaction, sample DNA is simultaneously fragmented and tagged with adapters, an optimized, limited-cycle PCR protocol amplifies tagged DNA and adds sequencing indexes. Individual libraries were assessed on the QIAxcel Advanced Automatic nucleic acid analyzer and then were quantitated through qPCR by the use of KAPA SYBR FAST qPCR Kits (Kapabio systems, Boston, US). The bacterial genome was sequenced on an Illumina HiSeq platform (Illumina, San Diego, CA, USA) as described previously [22]. Breseq v. 0.33.0 was used for comparative genome analyses [23], referencing the original genome of ATCC17978 (GenBank accession NZ_CP018664.1). Mutations were confirmed by PCR and Sanger sequencing.

Cloning, expression, and recombinant RsmG protein purification

The full-length coding sequences of *A. baumannii* ATCC17978 *rnaseI* (AUO97_RS04110) and *rsmG* (AUO97_RS15310) were amplified using DNA from *A. baumannii* ATCC17978 and cloned into the pYMAb2 vectors to generate pYMAb2-*rnaseI* and

pYMAb2-*rsmG*. Plasmids were verified by DNA sequencing and are listed in Table S2.

Bacterial expression and purification of His-tagged RsmG (RsmG-WT, RsmG Δ T, and RsmG(TTG)_{2→3}) were performed as described previously [24]. Briefly, the *rsmG* sequence (AUO97_RS15310) was amplified using DNA from *A. baumannii* ATCC17978/ACD9/HCD9, cloned into the pET28A vector to generate the pET28A-*rsmG*-WT/ pET28A-*rsmG* Δ T/ pET28A-*rsmG*(TTG)_{2→3} constructs, and transformed into competent BL21 (DE3) cells. Isopropyl- β -D-thiogalactoside was added to the bacterial suspension to a final concentration of 1 mM to induce target protein production. Details of protein purification are provided in the **Supplementary Methods**.

Minimum inhibitory concentration determination

The minimum inhibitory concentration (MIC) of the following antibiotics was determined by the broth microdilution method with cation-adjusted MH broth (Oxoid, Hampshire, UK): cefoperazone/sulbactam (1:1, CFU/SU), ceftazidime (CAZ), cefepime (FEP), cefiderocol (CFDC), imipenem (IPM), meropenem (MEM), colistin (COL), amikacin (AMK), and gentamicin (GEN). MIC values were interpreted according to the Clinical and Laboratory Standards Institute guidelines (CLSI) [25].

Quantitative biofilm assay

Biofilm formation on polystyrene was measured via crystal violet staining [26]. Each strain was cultivated overnight at 37°C, and the cultures were diluted 1:100 into 150 μ L MH broth in 96-well plates and incubated at 37°C for 24 h. The cultures were washed three times with PBS and stained with 0.1% crystal violet, washed with PBS, and 200 μ L 30% acetic acid was added to each well. The optical density at 550 nm (OD₅₅₀) of each well was quantified using a microplate reader.

Bacterial adherence and invasion assay

For bacterial adherence assay, *A. baumannii* was added to a monolayer of epithelial cells at an MOI of 100 and incubated in a 5% CO₂ atmosphere at 37°C for 1 h. For bacterial invasion assay, *A. baumannii* was added to THP-1 M ϕ cells at an MOI of 100 and incubated in a 5% CO₂ atmosphere at 37°C for 1 h. The cells were washed three times with PBS and a fresh culture medium containing 100 μ g/mL gentamicin was added, followed by incubation for 2 h. The cells were washed three times with PBS and lysed with 0.2% Triton X-100 for 20 min, and the lysate was plated on MH agar after gradient dilution. Details are provided in the **Supplementary Methods**.

Membrane permeability assay

Membrane permeability was measured using To-Pro-3 (Invitrogen, Thermo Fisher Scientific) and DiOC₂(3) (3, 3'-diethyloxycarbocyanineiodide) as described previously [27]. Membrane permeability was expressed as the ratio of To-Pro-3 fluorescence to green fluorescence or the frequency of To-Pro-3⁺ cells. Details are provided in the **Supplementary Methods**.

Bacterial capsule detection, surface polysaccharide extraction, and Alcian blue staining

Bacterial capsules were stained with Congo red and observed under a microscope (Olympus, Tokyo, Japan). Surface polysaccharides were extracted using the hot aqueous-phenol method [27]. Polysaccharide extracts were separated by sodium dodecyl sulfate-polyacrylamide gel electrophoresis and stained with Alcian blue (Sangon Biotech, Co., Ltd.).

Direct RNA sequencing and EpiNano-based m⁷G-modified site prediction

m⁷G-modified sites were predicted as described previously [28]. Briefly, *A. baumannii* total RNA samples were used to prepare RNA libraries for direct RNA sequencing; the sequence data were analyzed using EpiNano. Modification scores at each site were obtained for ATCC17978 and the *rsmG* mutant strains (*rsmG* Δ T and *rsmG*(TTG)_{2→3}). Details are provided in the **Supplementary Methods**.

In vitro m⁷G methyltransferase activity by LC-MS/MS

RNA probes derived from 16S rRNA of *A. baumannii* ATCC17978 were purchased from Beijing Tsingke Biotechnology Co., Ltd. *In vitro* methyltransferase activity assay was performed as described previously [29]. Briefly, a 50 μ L reaction mixture containing the RNA probe, recombinant protein (RsmG-WT, RsmG Δ T, and RsmG(TTG)_{2→3}), and SAM was incubated at 37°C for 3 h, and the reaction products were digested by nuclease P1 and alkaline phosphatase for QQQ LC-MS/MS analysis [30]. Total m⁷G and G contents were quantified based on standard curves (Figure S2 A–D) to calculate the m⁷G/G ratio. Details are provided in the **Supplementary Methods**.

In vitro translation assay

Cell-free translation of eGFP mRNA was performed as described previously [31]. Briefly, a homemade *Escherichia coli in vitro* transcription-translation PURE system was used to assess 70S ribosome activity. PURE

reaction mix (15 μ L), which translates the eGFP gene, was added to 70S ribosome (*rsmG*-WT, *rsmG* Δ T, and *rsmG*(TTG)_{2→3}). Protein synthesis was performed by incubation at 37°C (lid temperature 42°C), and eGFP fluorescence intensity was read at 0.5, 1, 1.5, and 2 h on a GloMax 20/20 luminometer (Promega).

Growth assay

Growth rates were determined in microplates using a Bioscreen C Microplate Reader (Oy Growth Curves Ab Ltd., Finland). The strains were cultured overnight at 37°C, and the cultures were diluted 1:100 into 200 μ L MH broth with or without the ferrous iron chelator, 2,2'-dipyridyl (DIP), and incubated at 37°C with shaking. Absorbance at 600 nm was measured at 5 min intervals. Each strain was assayed in three independent cultures and three separate experiments. Growth was determined by calculating the area under the growth curve [32].

Transcriptome analysis of *A. baumannii* *rsmG* and *rnaseI* mutants

To investigate the role of *rnaseI* and *rsmG* in antibiotic resistance, RNA-seq of *A. baumannii* ATCC17978, *rnaseI* Δ , *rsmG* Δ T, and *rsmG*(TTG)_{2→3} was performed as described previously [33]. Briefly, *A. baumannii* ATCC17978, *rnaseI* Δ , *rsmG* Δ T, and *rsmG*(TTG)_{2→3} total RNA were subjected to RNA-sequencing, and genes differentially expressed in the *rsmG* and *rnaseI* mutants were screened. Details are provided in the **Supplementary Methods**.

RNA preparation, quantitative reverse transcription-PCR, and mRNA stability measurement

Total RNA was extracted, and RT-PCR was performed following the manufacturer's instructions (Cat. No. RR037A; TaKaRa, Tokyo, Japan). TB Green Premix Ex Taq II (Cat. No. RR820A; TaKaRa, Tokyo, Japan) was used for signal detection, followed by real-time PCR analysis (Roche LightCycler480; Roche Molecular Systems, Basel, Switzerland) of gene expression levels; the primer sequences are listed in Table S3. For mRNA stability measurement, bacterial cultures were harvested at 0, 1, and 3 min after rifampicin addition (1 mg/mL), and total RNA samples were prepared and subjected to qRT-PCR. Details are provided in the **Supplementary Methods**.

Statistical analysis

Data are expressed as means \pm standard deviations. Comparisons between two groups were performed using two-tailed unpaired Student's *t*-tests. One-way

analysis of variance was used for multiple-group comparisons. Two-way repeated measures analysis of variance was used to compare changes in a single variable over time in each group. Statistical analyses were performed using Prism v. 9.0 (GraphPad Software, San Diego, CA). *P* < 0.05 was considered to indicate statistical significance.

Results

The emergence of morphological and phenotypic diversity

We generated four evolved *A. baumannii* populations (all from the same ancestral colony of ATCC17978) that adapted to the antagonistic interaction with A549 and HBE cells. The populations (A1 to A3 and H1 to H3) evolved in a complete culture medium with A549 or HBE cells at an MOI of 1:1 (10^6 *A. baumannii* to 10^6 cells). Populations (A4 to A6 and H4 to H6) evolved under identical conditions in the absence of cells and were used as the controls. Bacteria from A1-A6 and H1-H6 were streaked on plates, and a randomly selected colony was cultured in liquid medium (Figure 1A). These colonies are hereafter referred to as ASD3/ASD6/ASD9/ACD3/ACD6/ACD9 and HSD3/HSD6/HSD9/HCD3/HCD6/HCD9 (Table S4).

Adaptation of *A. baumannii* in the presence of epithelial cells was characterized by mucoid phenotype emergence. After 3 days, mucoid colonies were observed in populations co-cultured with A549 and HBE cells. This was not observed in the control groups (Figure 1 and Figure S1). Congo red capsule staining showed a thickened capsule in colonies from evolved populations (ACD9 and HCD9) compared to those from control populations (ASD9 and HSD9). A sedimentation assay of microviscosity showed that the OD₆₀₀ of the supernatant of evolved strains (ACD9 and HCD9) was higher than that of the control strains (ASD9 and HSD9). Crystal violet staining showed that the evolved strains had considerably weaker biofilm formation than the control strains. Regarding cell adherence and internalization, the evolved strains showed less adhesion to epithelial cells and less internalization into macrophages than the control strains. The evolved strains showed significantly different antibiotic susceptibilities, and their resistance to cephalosporins increased significantly (Table 1).

Identification and investigation of genetic mutations associated with morphological and phenotypic diversity

To detect mutations, the genomes of ACD9 and HCD9 were subjected to whole genome sequencing (WGS). Three and two mutations were detected in

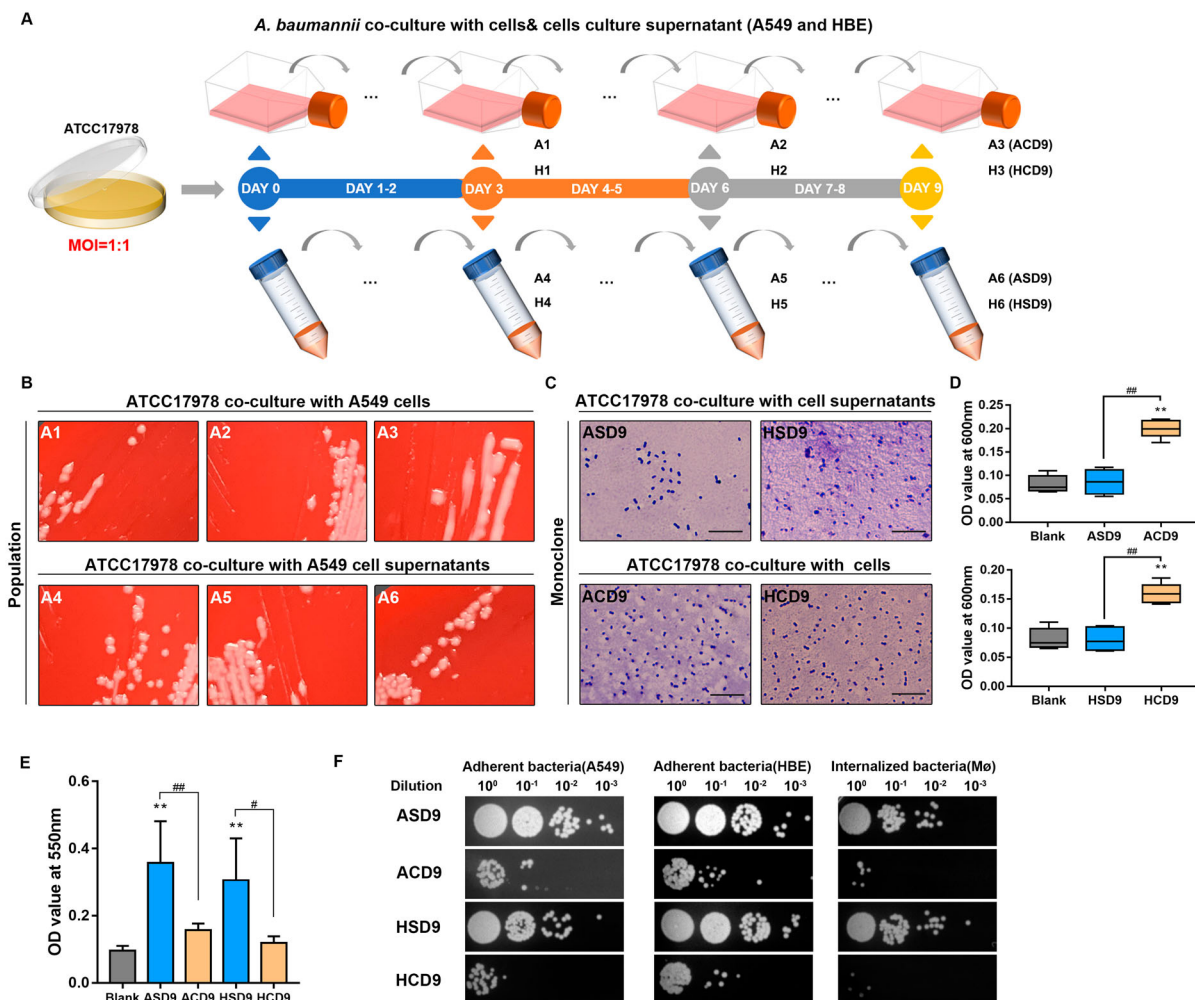


Figure 1. Evolution experiment and phenotypic characterization. (A) Pathogen–host cell co-culture-based laboratory evolution experiment. (B) Representative images of the morphological diversity of *A. baumannii* populations adapted to pulmonary epithelial cells (A549 and HBE). (C) Representative Congo red-stained images of capsules of colonies (ASD9/ACD9/HSD9/HCD9) derived from evolved strains. Scale bar, 10 μ m (D) OD₆₀₀ values of culture supernatants. (E) Biofilm formation is revealed by crystal violet staining. (F) Adherence to epithelial cells and internalization by macrophages. Data are from at least three independent experiments; error bars represent standard deviations. ** $P < 0.01$ vs. blank group, ## $P < 0.01$, # $P < 0.05$.

ACD9 and HCD9, respectively, and confirmed by Sanger sequencing (Table 2). *ptk* (AUO97_RS06965) and *rsmG* (AUO97_RS15310) were mutated in ACD9 and HCD9, and *rnaseI* (AUO97_RS04110) was mutated only in ACD9. The mutation in *ptk* resulted in a substitution of valine for glutamic acid at amino acid 653 (*ptk* V653E). *rsmG* harboured a missense mutation (584/633nt) and glutamine insertion (175/633nt). The mutation in *rnaseI* (*rnaseI* Δ) resulted in premature termination of translation (*rnaseI*^{M122*}).

Next, the impact of each mutation on morphological and phenotypic diversity was investigated (Figure 2). We introduced four mutations into the genome of the parental strain ATCC17978 to generate four mutant strains. The effect of each mutation was determined by evaluating mucoid phenotype and antibiotic susceptibility. Only *ptk* V653E showed a distinct mucoid phenotype, as indicated by a thickened capsule and increased microviscosity, decreased adhesion to epithelial cells and internalization into macrophages, and decreased biofilm formation. The *rsmG* and *rnaseI* mutations but

not *ptk* mutations significantly altered antibiotic susceptibility (Table S5). ATCC17978 and the *rsmG* and *rnaseI* mutations (*rsmG* Δ T, *rsmG*(TTG)₂₋₃, and *rnaseI* Δ) were transformed with a plasmid encoding WT *rsmG* and *rnaseI*, which restored their susceptibility to cephalosporins (Table S6).

Enhancement of capsular exopolysaccharide chain length in *ptk* mutation mediates mucus phenotype and reduces bacterial adhesion and internalization

Next, we replaced the mutated *ptk* in ACD9 and HCD9 with the WT *ptk*, thus generating the revertant mutants ACD9/*ptk*-WT and HCD9/*ptk*-WT (Figure 2). Compared to their parental strains, the two revertant mutants lacked a mucoid phenotype and had a thinner capsule and increased epithelial cell adhesion and macrophage internalization. SDS-PAGE and Alcian blue staining showed that the lysates of ACD9, HCD9, and *ptk* V653E had a very high-molecular-

Table 1. Antimicrobial susceptibility of ATCC17978 and *in vitro* evolved strains

Strains	MIC (mg/L)								
	AMK	GEN	FEP	CFU/SU	CAZ	CFDC	MEM	IPM	COL
ASD9	2	1	8	1	4	0.125	0.25	0.125	0.5
ACD9	4	1	>128	64	>128	8	2	0.5	0.25
HSD9	2	1	8	1	4	0.125	0.25	0.25	0.5
HCD9	2	2	64	16	32	2	1	0.25	0.5
ATCC17978	2	0.5	4	1	2	0.125	0.25	0.25	0.5
ATCC25922	2	0.5	0.03	0.25	0.125	0.25	0.03	0.125	0.06

Note: MIC: Minimum inhibitory concentration; AMK: amikacin; GEN: gentamicin; FEP: cefepime; CFU/SU: cefoperazone/sulbactam (1:1); CAZ: ceftazidime; CFDC: cefiderocol; MEM: meropenem; IPM: imipenem; COL: colistin.

weight (HMW) polysaccharide that replaced the capsular polysaccharide band of the WT. This polysaccharide was also present in the culture supernatant. The polysaccharide bands of the two revertant mutants were similar to those of the WT. Therefore, *ptk* mutation increased the capsule polymer chain length. To investigate the effect of the extended polymer chain on host cells, we determined the mRNA levels of proinflammatory cytokines, including IL-6, IL-8, and TNF- α in A549, HBE, and THP-1 M ϕ . The IL-6, IL-8, and TNF- α transcript levels were significantly upregulated in the *ptk* V653E-infected groups, compared to the control and WT-infected groups.

The m⁷G524 deficiency caused by *rsmG* mutation induces antibiotic resistance

The m⁷G modification of 16S rRNA in the presence or absence of *rsmG* mutation was detected by Oxford Nanopore Technologies (ONT), a third-generation sequencing technology. m⁷G modification of G524 and G526 (replacement of guanosine with adenosine at nucleotide 520 in the 16S rRNA of *A. baumannii*) in 16S rRNA was missing in the *rsmG* mutant (Figure 3A). RsmG mediates m⁷G modification of nucleotide 527 in the 16S rRNA of *E. coli* (corresponds to G524 of *A. baumannii*) (Figure 3B). Consistent with previous studies, strains harbouring the *rsmG* mutation exhibited elevated MICs to streptomycin (Table S7). Next, an *in vitro* methyltransferase activity assay was performed to determine m⁷G activity and to verify modification sites for synthetic RNA probes with or without potential modification sites (obtained from ONT). Total m⁷G and G contents were measured via LC-MS/MS and quantified based on standard curves (Figure 3C). The RsmG mutant protein (RsmG Δ T, RsmG(TTG)₂₋₃) showed no methyltransferase activity with RNA probe 1 (WT), whereas WT RsmG exhibited

methyltransferase activity (Figure 3D). Therefore, *rsmG* mutation results in the loss of RsmG methylation activity. RNA probes 2 and 4 (524G to 524A in the consensus sequence) resulted in inefficient methylation compared to RNA probes 1 and 3 (524G) (Figure 3E and Figure S2). In addition, the m⁷G modification was downregulated by 526G to 526A (RNA Probe 3) but was significantly higher than that of RNA probes 2 and 4 (Figure S2F). The secondary structure of RNA Probe 3 (526G to 526A) changed significantly compared to RNA Probe 1 (WT), potentially affecting methylation and indicating that RsmG has site specificity (Figure S1B). These results led us to hypothesize that *rsmG* mutations increase protein synthesis. Therefore, we measured the *in vitro* translational activity of ribosomes from the WT and *rsmG* mutant strains, using eGFP mRNA as a template. Ribosomes from the *rsmG* mutants (*rsmG* Δ T, *rsmG*(TTG)₂₋₃) exhibited higher eGFP synthetic activity than the WT (Figure 3F). Ribosomes from *rsmG*-complemented strains (*rsmG* Δ T/pYMAb2-*rsmG* and *rsmG*(TTG)₂₋₃/pYMAb2-*rsmG*) showed decreased eGFP synthetic activity compared to the corresponding *rsmG* mutant strains (*rsmG* Δ T/pYMAb2 and *rsmG*(TTG)₂₋₃/pYMAb2) (Figure 3G and H). Therefore, *rsmG* mutations resulted in m⁷G524 deficiency, which increased translation efficiency and acted as a global regulator.

The *rnaseI* mutation affects outer membrane permeability and efflux pump expression

Transcriptomic analysis was performed to explore the mechanism of *rnaseI* mutation-mediated antibiotic resistance. The transcriptome of the WT and *rnaseI* Δ A strains revealed upregulation of four genes encoding RND efflux transporters, which mediate antibiotic transport, and upregulation of five genes involved in outer membrane formation (Figure 4A and B). We hypothesized that modulation of nucleotide homeostasis mediates some of the transcriptional and phenotypic changes observed in *rnaseI* Δ A, therefore, we performed mRNA stability assays. The mRNA stability of RND efflux transporter-related genes and outer membrane protein/lipoprotein synthesis-related genes in *rnaseI* Δ A were significantly higher than that of the WT after

Table 2. Mutations acquired by evolved clones identified through whole genome re-sequencing (WGS).

Strains	Gene	Mutation	Annotation
ACD9	<i>rnaseI</i>	Coding (320/663 nt)	Δ 1 bp
	<i>rsmG</i>	Coding (175/633 nt)	(TTG) ₂₋₃
	<i>ptk</i>	T \rightarrow A	V653E (GTG \rightarrow GAG)
HCD9	<i>rsmG</i>	Coding (584/633 nt)	Δ 1 bp
	<i>ptk</i>	T \rightarrow A	V653E (GTG \rightarrow GAG)

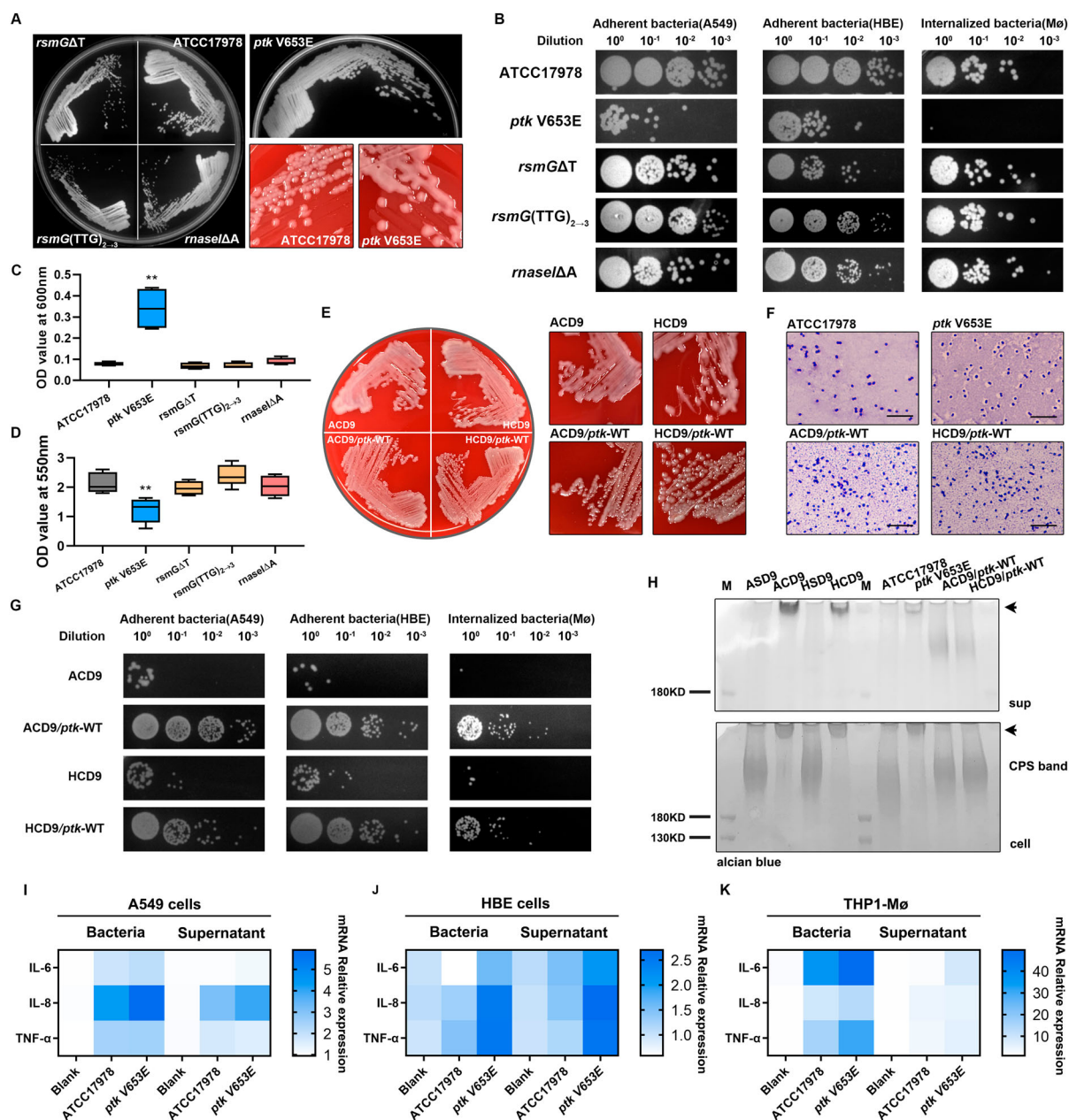


Figure 2. *ptk* mutation induces the mucoid phenotype and reduces adhesion and internalization. (A) Representative images of morphological diversity of ATCC17978 and its mutant strains (*ptk* V653E, *rsmG* Δ T, *rsmG*(TTG)₂₋₃, and *rnaseI* Δ A). (B) Adherence to epithelial cells and internalization by macrophages of ATCC17978 and its mutant strains. (C) OD₆₀₀ values of culture supernatants of ATCC17978 and its mutant strains. (D) Biofilm formation by ATCC17978 and its mutant strains as revealed by crystal violet staining. (E) Representative images of morphological diversity of the evolved and *ptk*-WT complemented strains. (F) Representative Congo red-stained images of the capsules of evolved strains and *ptk*-WT complemented strains. Scale bar, 10 μ m. (G) Adherence to epithelial cells and internalization by macrophages of evolved strains and *ptk*-WT complemented strains. (H) Capsular exopolysaccharide stained with Alcian blue (sup supernatant, arrows HMW exopolysaccharides). (I–K) IL-6, IL-8, and TNF- α mRNA levels in A549 cells (I), HBE cells (J), and THP-1 derived macrophages (K) at 3 h after infection. ***P* < 0.01 vs. ATCC17978 group.

transcriptional repression by rifampicin (Figure 4C and D). Next, we examined the effect of carbonyl cyanide 3-chlorophenylhydrazone (CCCP; efflux pump inhibitor) on MIC values. CCCP reduced the MIC values of *rnaseI* Δ A (Table S8). Scanning electron microscopy (SEM) showed that the outer membrane morphologies of the ACD9 and *rnaseI* Δ A strains were significantly changed compared to the ASD9 and ATCC17978 WT strains. Evolved and mutant cells were of heterogeneous shapes rather

than the homogenous shape of the parental isolate (Figure 4E). In addition, the outer membrane permeability was reduced in ACD9 compared to ASD9, and in the *rnaseI* Δ A strain compared to the WT strain, as measured according to the positive cell frequency (Figure 4F) and fluorescence intensity (Figure 4G). Therefore, overexpression of RND efflux transporters and changes in outer membrane morphology and permeability are implicated in the antibiotic resistance of the *rnaseI* Δ A strain.

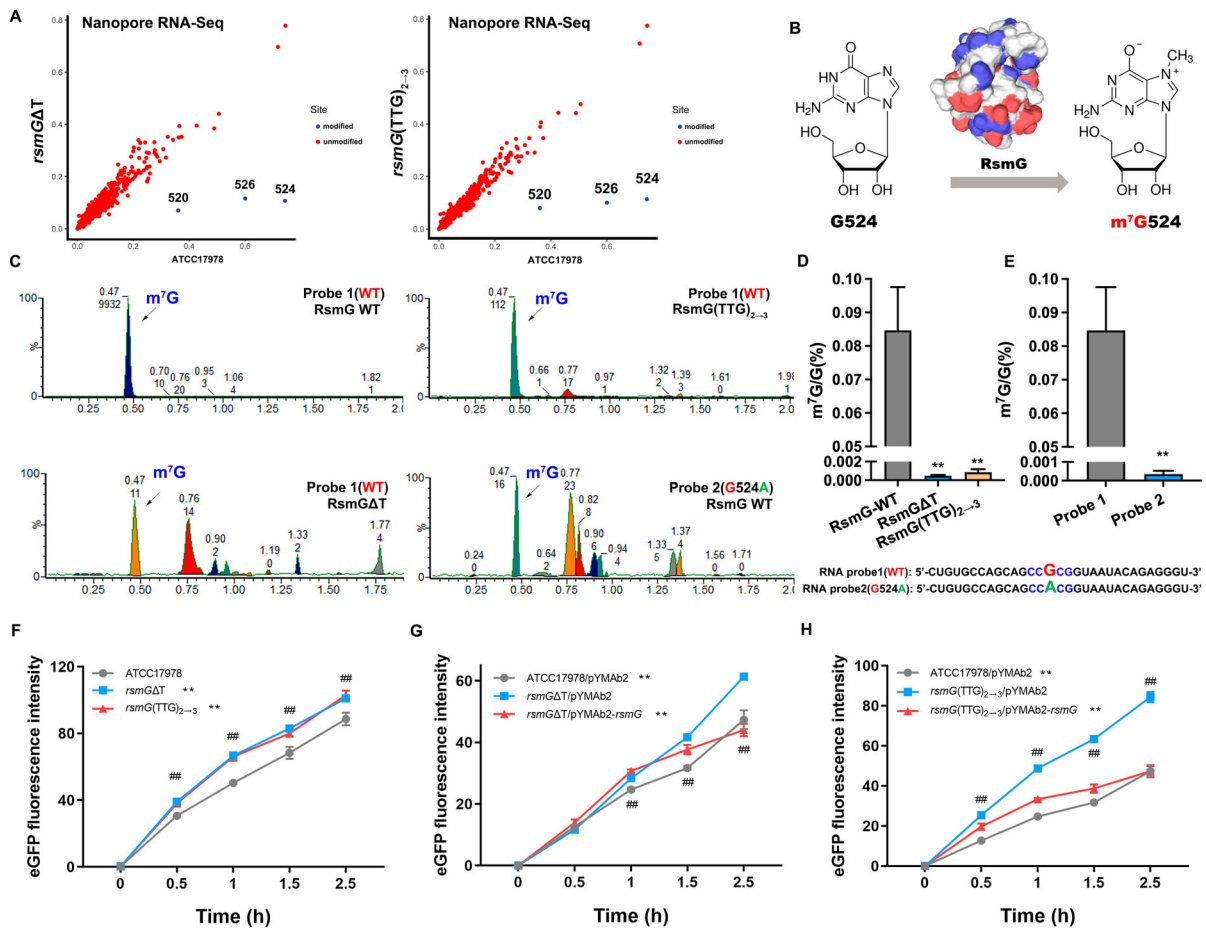


Figure 3. m^7G524 deficiency caused by *rsmG* mutation increases ribosomal translation efficiency. (A) Prediction of m^7G modification site in *rsmG* mutant strains by third-generation sequencing. (B) RsmG mediated m^7G modification of nucleotide 524 in the 16S rRNA of *A. baumannii*. (C) *In vitro* methyltransferase activity using 16S rRNA probes and RsmG protein, with detection of m^7G and G by LC-MS/MS. (D and E) m^7G/G ratio. (F–H) 70S ribosome activity of *rsmG* mutant (F) and complemented strains (G and H) by *in vitro* translation assay. ** $P < 0.01$ vs. RsmG-WT (Probe 1, ATCC17978, *rsmGΔT*/pYMAb2 or *rsmG(TTG)₂₋₃*/pYMAb2) groups, ## $P < 0.01$.

The *rsmG* and *rnaseI* mutation impairs iron acquisition, which may mediate resistance to cefiderocol

The *rsmG* and *rnaseI* mutants (*rsmGΔT*, *rsmG(TTG)₂₋₃*, and *rnaseIΔA*) showed downregulation of *bauB*, *bauE*, *bauF*, *basB*, *basC*, *basD*, *basE*, *basF*, *basG*, and *basJ* (Figure 5A). These genes are linked to siderophore and siderophore-receptor biosynthesis. We hypothesized that downregulated expression of these genes may suppress iron acquisition and utilization. In the completed medium, the growth of the *rsmG* and *rnaseI* mutants was not inhibited compared to the WT (Figure 5B and H), whereas the *rsmG* and *rnaseI* mutants displayed significant growth restriction in an iron-limited medium (containing the ferrous iron chelator 2,2'-dipyridyl; DIP) (Figure 5C, D, and H). In the presence of 100 μ M DIP, only the *rsmGΔT*/pYMAb2-*rsmG* strain partially recovered from growth restriction (Figure 5F, and I–K). In the presence of 200 μ M DIP, the growth of the *rnaseI* and *rsmG*-complemented strains partially recovered (Figure 5G, and I–K). Mutations in these genes impaired bacterial utilization of iron,

possibly explaining the reduction in cefiderocol susceptibility.

Discussion

Bacterial evolution from a commensal to a pathogen may occur by the acquisition of new gene via horizontal gene transfer (gain of function) or accumulation of pathoadaptive mutations (change in function) [34,35]. For example, macrophage-adapted *E. coli* exhibit increased intracellular survival and delayed phagosome maturation due to a single IS1 insertion upstream of *yrjF* [3]. The loss of function of *muca* in *Pseudomonas aeruginosa* results in an increased ability to escape phagocytosis and pulmonary clearance [36]. The lung is the main colonization and infection site of *A. baumannii*, an opportunistic pathogen mainly in patients on mechanical ventilation [7]. The airway epithelium is the first line of defense against invasion by pathogenic microorganisms, and epithelial cells trigger the host inflammatory response [17]. Therefore, the acquisition of adaptive mutations is essential for *A. baumannii*

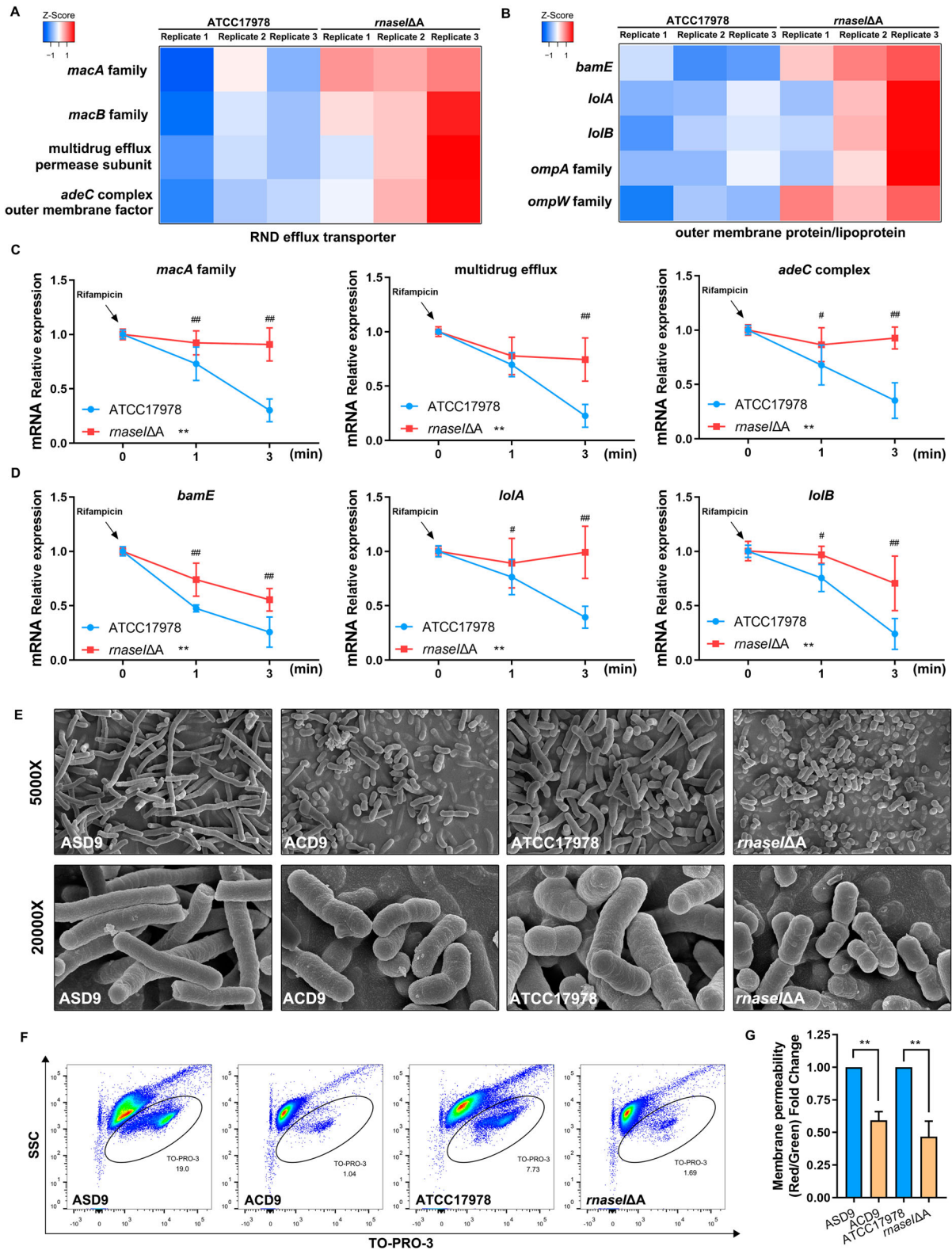


Figure 4. *rnaseI* mutation affects outer membrane permeability and efflux pump expression. (A) Heatmap of RND efflux transporter gene expression. (B) Heatmap of outer membrane formation gene expression. (C and D) mRNA stability of RND efflux transporter-related genes (C) and outer membrane protein/lipoprotein synthesis-related genes (D) in *rnaseI*ΔA compared to ATCC17978. (E) Representative images of the morphology of the evolved and *rnaseI* WT/ΔA strains by scanning electron microscopy (SEM). (F and G) Outer membrane permeability was measured via flow cytometry – the percentage of TO-PRO-3 positive cells (F) and adjusted fluorescence intensity (G). ***P* < 0.01, **P* < 0.05 vs. ATCC17978 or ASD9 group, ##*P* < 0.01, #*P* < 0.05.

persistence. It is shown that *A. baumannii* can very easily acquire and lose genes [37]. Several pathogenic bacteria have evolved to survive and indeed take advantage of the host environment [38]. In this study, we

induced the evolution of *A. baumannii* *in vitro* with two pulmonary epithelial cell lines. Epithelial cell-adapted *A. baumannii* exhibited a mucoid phenotype and enhanced antibiotic resistance, and several

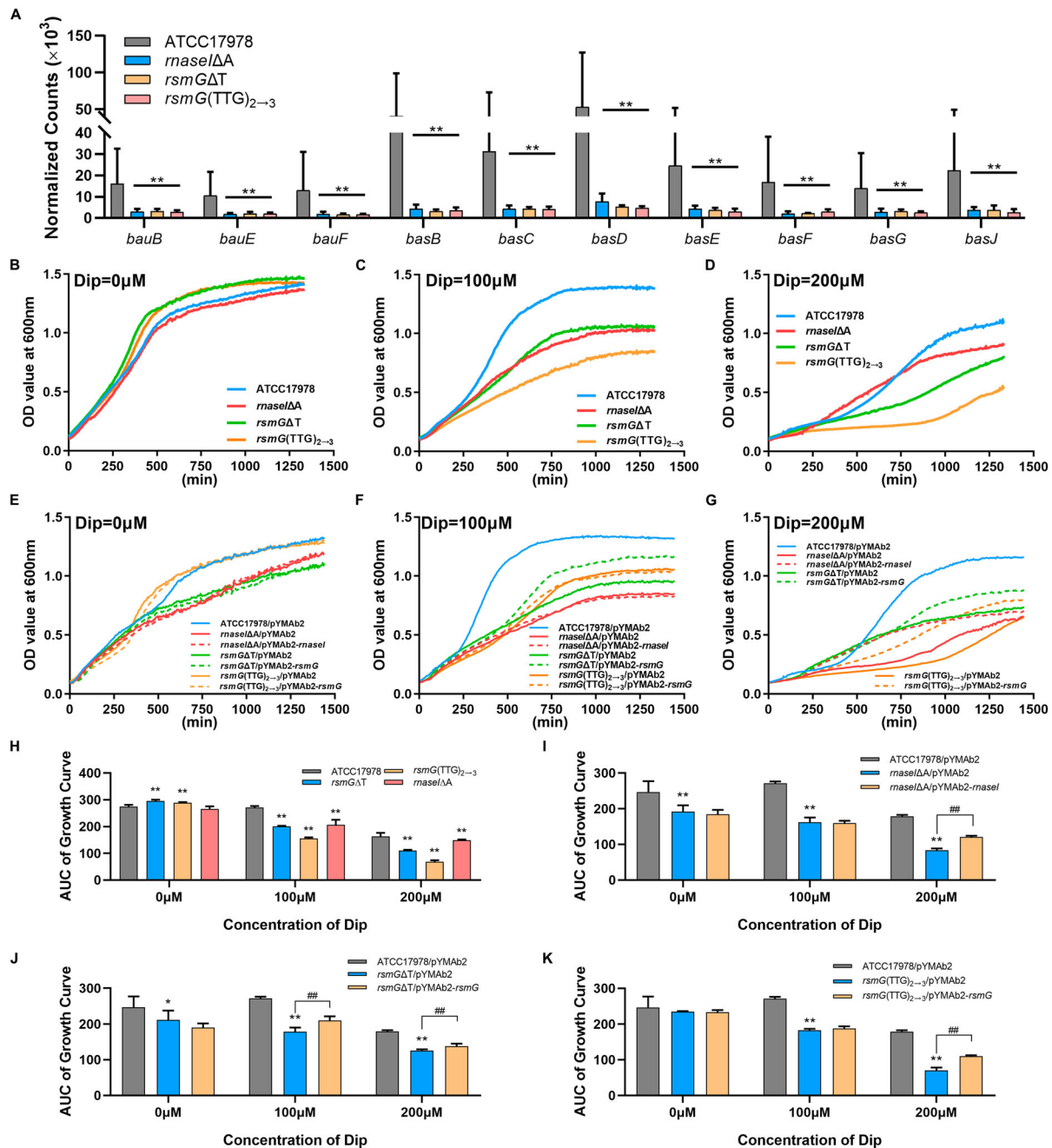


Figure 5. *rsmG* and *rnasel* mutations impair bacterial iron acquisition and utilization. (A) Siderophore and siderophore receptor gene expression data in *rsmG* and *rnasel* mutants. (B–G) Growth curves of the mutants (B–D) and their complemented strains (E–G) in the presence or absence of the ferrous iron chelator 2,2'-dipyridyl (DIP). (H–K) Areas under the growth curves (AUC) of the mutants (H) and their complemented (I–K) strains in the presence or absence of DIP. ** $P < 0.01$, * $P < 0.05$ vs. ATCC17978 or ATCC17978/pYMAb2 group, ## $P < 0.01$, # $P < 0.05$.

gene mutations and deletions (Table S9) were found. The mucoid phenotype was characterized by reduced adhesion to epithelial cells and internalization by macrophages. The antibiotic resistance adaptation was associated with the overproduction of efflux pumps and reduced outer-membrane permeability (Figure 6).

In a previous study, we found that clinical isolates from sputum showed enhanced resistance and morphological changes after within-host evolution [39]. In that study, we identified mutations in *ptk* that caused mucoid conversion and decreased adherence and internalization, promoting dissemination.

Macrophage- and neutrophil-adapted *A. baumannii* also undergo mucoid conversion and *ptk* mutation (unpublished data). The K locus, which encompasses *ptk*, is responsible for capsule biosynthesis, and *ptk* mutants produce very HMW polysaccharides [40]. Our data confirm that *ptk* mutations trigger the production of HMW exopolysaccharides, which have a pro-inflammatory effect on host cells. Capsular exopolysaccharide is important for soft tissue infection, defense against serum factor-mediated killing, and biofilm formation [41]. Therefore, the acquisition of a mucoid phenotype promotes the

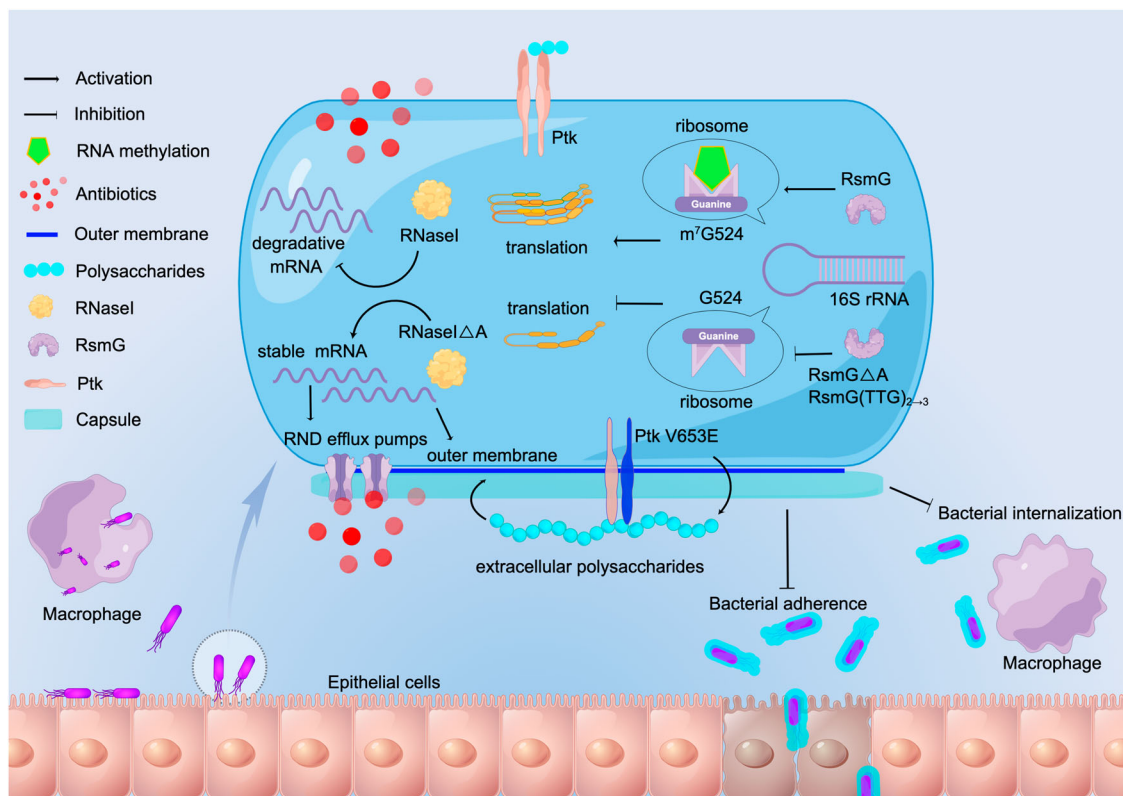


Figure 6. Proposed mechanism of *A. baumannii* pathoadaptation to epithelial cells. In *A. baumannii*, mutation of *ptk* mediates mucoid conversion and reduces adhesion and internalization. Mutations of *rsmG* and *rnaseI* involve in antibiotic resistance, and m⁷G524 deficiency in 16S rRNA caused by *rsmG* mutation increases ribosomal translation efficiency and may act as global regulators, and *rnaseI* mutation affects outer membrane permeability and efflux pump expression by modulating RNA metabolism. (By Figdraw, www.figdraw.com).

dissemination and persistence of *A. baumannii* in the host.

Antibiotic resistance contributes to the persistence of *A. baumannii* in the host [39] and is an adaptive response to stress [21]. In this study, epithelial cell-adapted *A. baumannii* showed enhanced resistance to ceftazidime, cefoperazone/sulbactam, cefepime, and cefiderocol, as a result of mutations to *rsmG* and *rnaseI* (linked to RNA modification and metabolism). *rsmG*, which encodes S-adenosylmethionine (SAM)-dependent 16S rRNA methyltransferase, is involved in 7-methylguanosine modification (m⁷G) of the 530 loops of 16S rRNA in a variety of Gram-negative bacteria [42,43]. In this study, mutations in *rsmG* resulted in the loss of the m⁷G modification of 16S rRNA in *A. baumannii*, and the modification site was G524 of 16S rRNA. We excluded G526 as a potential methylation modification site because the RNA probe retained the m⁷G modification after the change from 526G to 526A. Therefore, the reduction of the m⁷G/G ratio was likely related to the altered secondary structure of RNA probe 3. *RsmG* mutation-associated loss of m⁷G modification mediates low-level streptomycin resistance [42,43]. In this study, *rsmG* mutation reduced susceptibility to several β -lactams, however, the resistance mechanism is unknown. RNA-seq revealed no resistance mechanism. The universally

conserved 530 loops of 16S rRNA is crucial for translation [44,45]. Loss of the m⁷G modification may affect ribosomal function [46], and the translation efficiency and fitness of bacterial pathogens [47]. Therefore, we hypothesized that the *RsmG* mutation enhances β -lactam resistance by affecting ribosome function and protein translation. Indeed, *rsmG* mutation increased ribosomal translation efficiency, a rapid-response mechanism to environmental stress [48,49]. Stress can reduce the overall protein translation capacity of bacteria [50], hampering their survival. Maintenance of translation efficiency guarantees timely synthesis of stress-responsive proteins, enabling long-term survival during colonization and infection [51]. Therefore, *rsmG* mutation-mediated upregulation of protein translation efficiency may promote bacterial survival under β -lactam stress.

β -lactam tolerance can also be mediated by overexpression of genes encoding efflux pumps and outer-membrane changes. Indeed, our data suggest that these were altered by *rnaseI* mutation. RNase I regulate bacterial biofilm formation, motility, acid resistance, β -lactam tolerance, and nucleotide metabolism [52]. Under stress conditions, periplasmic RNase I enter the cell, leading to extensive RNA degradation [53]. In this study, the mRNA stability of RND efflux pumps and outer membrane genes was

upregulated by *rnaseI* mutation, enhancing the expression of RND efflux pumps, changing the morphology of the outer membrane, and decreasing its permeability, leading to β -lactam resistance. In addition, impaired iron utilization caused by the *rsmG* and *rnaseI* mutations promoted resistance to cefiderocol. This is unlike previously reported cefiderocol resistance mechanisms, such as mutations in genes encoding iron transport-related proteins and the transfer of an extended-spectrum β -lactamase-encoding gene [54,55]. This study demonstrates a mutagenic role for host factors previously thought to be unsusceptible to resistance by mutation.

Conclusion

A. baumannii adapted to host-associated selective pressures during 9 days of co-culture with epithelial cells. Mucoid clones with β -lactam resistance and the ability to evade adherence and phagocytosis rapidly emerged. Our data reveal the complex influence of pulmonary epithelial cells on *A. baumannii* pathoadaptation, implicating the host-microbe interaction in *A. baumannii* survival and persistence. This pathoadaptation could explain the emergence of antibiotic resistance and tissue translocation in patients infected with *A. baumannii*. Our findings provide insight into the effect of the host response on the evolution of *A. baumannii*.

Acknowledgements

The work was supported by the National Natural Science Foundation of China (82072313, 31770142, 81971897) and the National Science Foundation of China International Cooperation and Exchange Programme (81861138054). We are grateful to Dr. Fengqin Wang from College of Animal Sciences, Zhejiang University for her great support to this work.

Authors' contributions

W. Z. and Y.S.Y. wrote the main manuscript text, X.T.H., H.Z., and Z.H.Z. designed this study, Y.Y., J.T.H., J.F.W., L.L., M.S.G., Y.F., and Y.S. participated in part of the experiments, H.C., J.Z.L., X.T.H., and J.Z.L. revised the manuscript, Y.Y. and X.C.L. analyzed the data.

Data availability

The complete genome sequences of the evolved strains (ACD9 and HCD9) were deposited in NCBI under BioProject No. PRJNA867505. The RNA-seq data of *A. baumannii* ATCC17978, *rnase I*, and *rsmG* mutants were deposited in NCBI under BioProject No. PRJNA867119. The direct RNA-seq (ONT) data of

A. baumannii rsmG WT/mutants were deposited in NCBI under BioProject No. PRJNA882509.

Disclosure statement

No potential conflict of interest was reported by the author(s).

Funding

This work was supported by National Natural Science Foundation of China [grant number: 31770142,81861138054, 81971897,82072313].

ORCID

Wang Zhang  <http://orcid.org/0000-0002-9830-8104>

Hua Zhou  <http://orcid.org/0000-0001-6397-3203>

Yunsong Yu  <http://orcid.org/0000-0003-2903-918X>

Xiaoting Hua  <http://orcid.org/0000-0001-8215-916X>

References

- [1] Olive AJ, Sasseti CM. Metabolic crosstalk between host and pathogen: sensing, adapting and competing. *Nat Rev Microbiol.* 2016 Apr;14(4):221–234.
- [2] Gatt YE, Margalit H. Common adaptive strategies underlie within-host evolution of bacterial pathogens. *Mol Biol Evol.* 2021 Mar 9;38(3):1101–1121.
- [3] Proenca JT, Barral DC, Gordo I. Commensal-to-pathogen transition: one-single transposon insertion results in two pathoadaptive traits in *Escherichia coli* -macrophage interaction. *Sci Rep.* 2017 Jul 3;7(1):4504.
- [4] Diaz Caballero J, Clark ST, Coburn B, et al. Selective sweeps and parallel pathoadaptation drive *Pseudomonas aeruginosa* evolution in the cystic fibrosis lung. *mBio.* 2015 Sep 1;6(5):e00981-15.
- [5] Mwangi MM, Wu SW, Zhou Y, et al. Tracking the in vivo evolution of multidrug resistance in *Staphylococcus aureus* by whole-genome sequencing. *Proc Natl Acad Sci U S A.* 2007 May 29;104(22):9451–9456.
- [6] Magret M, Lisboa T, Martin-Loeches I, et al. Bacteremia is an independent risk factor for mortality in nosocomial pneumonia: a prospective and observational multicenter study. *Critical Care (London, England).* 2011;15(1):R62.
- [7] Brotfain E, Borer A, Koyfman L, et al. Multidrug resistance *Acinetobacter* bacteremia secondary to ventilator-associated pneumonia: risk factors and outcome. *J Intensive Care Med.* 2017 Oct;32(9):528–534.
- [8] Eijkelkamp BA, Stroehel UH, Hassan KA, et al. H-NS plays a role in expression of *Acinetobacter baumannii* virulence features. *Infect Immun.* 2013 Jul;81(7):2574–2583.
- [9] Zhang W, Zhou H, Jiang Y, et al. *Acinetobacter baumannii* outer membrane protein A induces pulmonary epithelial barrier dysfunction and bacterial translocation through the TLR2/IQGAP1 axis. *Front Immunol.* 2022;13:927955.
- [10] Geisinger E, Huo W, Hernandez-Bird J, et al. *Acinetobacter baumannii*: envelope determinants that control drug resistance, virulence, and surface

- variability. *Annu Rev Microbiol.* 2019 Sep 8;73:481–506.
- [11] Campos MA, Vargas MA, Regueiro V, et al. Capsule polysaccharide mediates bacterial resistance to antimicrobial peptides. *Infect Immun.* 2004 Dec;72(12):7107–7114.
- [12] Llobet E, Tomas JM, Bengoechea JA. Capsule polysaccharide is a bacterial decoy for antimicrobial peptides. *Microbiology (Reading).* 2008 Dec;154(Pt 12):3877–3886.
- [13] Jones A, Georg M, Maudsdotter L, et al. Endotoxin, capsule, and bacterial attachment contribute to *Neisseria meningitidis* resistance to the human antimicrobial peptide LL-37. *J Bacteriol.* 2009 Jun;191(12):3861–3868.
- [14] Smith MG, Gianoulis TA, Pukatzki S, et al. New insights into *Acinetobacter baumannii* pathogenesis revealed by high-density pyrosequencing and transposon mutagenesis. *Genes Dev.* 2007 Mar 1;21(5):601–614.
- [15] Wong D, Nielsen TB, Bonomo RA, et al. Clinical and pathophysiological overview of *Acinetobacter* infections: a century of challenges. *Clin Microbiol Rev.* 2017 Jan;30(1):409–447.
- [16] McConnell MJ, Actis L, Pachon J. *Acinetobacter baumannii*: human infections, factors contributing to pathogenesis and animal models. *FEMS Microbiol Rev.* 2013 Mar;37(2):130–155.
- [17] Naumann M. Nuclear factor-kappa B activation and innate immune response in microbial pathogen infection. *Biochem Pharmacol.* 2000 Oct 15;60(8):1109–1114.
- [18] Mortensen BL, Skaar EP. Host-microbe interactions that shape the pathogenesis of *Acinetobacter baumannii* infection. *Cell Microbiol.* 2012 Sep;14(9):1336–1344.
- [19] Wright MS, Jacobs MR, Bonomo RA, et al. Transcriptome remodeling of *Acinetobacter baumannii* during infection and treatment. *mBio.* 2017 Mar 7;8(2):e02193-16.
- [20] Quinn B, Rodman N, Jara E, et al. Human serum albumin alters specific genes that can play a role in survival and persistence in *Acinetobacter baumannii*. *Sci Rep.* 2018 Oct 3;8(1):14741.
- [21] Martinez J, Fernandez JS, Liu C, et al. Human pleural fluid triggers global changes in the transcriptional landscape of *Acinetobacter baumannii* as an adaptive response to stress. *Sci Rep.* 2019 Nov 21;9(1):17251.
- [22] Hua X, He J, Wang J, et al. Novel tigecycline resistance mechanisms in *Acinetobacter baumannii* mediated by mutations in *adeS*, *rpoB* and *rrf*. *Emerg Microbes Infect.* 2021 Dec;10(1):1404–1417.
- [23] Deatherage DE, Barrick JE. Identification of mutations in laboratory-evolved microbes from next-generation sequencing data using breseq. *Methods Mol Biol.* 2014;1151:165–188.
- [24] Li Y, Zhu Y, Zhou W, et al. *Alcaligenes faecalis* metallo- β -lactamase in extensively drug-resistant *Pseudomonas aeruginosa* isolates. *Clin Microbiol Infect.* 2022 Jun;28(6):880.e1–880.e8.
- [25] CLSI. Performance standards for antimicrobial susceptibility testing. 29th ed. Wayne (PA): Clinical and Laboratory Standards Institute; 2019; p. 1–282.
- [26] Hu L, Shi Y, Xu Q, et al. Capsule thickness, not biofilm formation, gives rise to Mucoid *Acinetobacter baumannii* phenotypes that are more prevalent in long-term infections: a study of clinical isolates from a hospital in China. *Infect Drug Resist.* 2020;13:99–109.
- [27] Xu Q, Chen T, Yan B, et al. Dual role of *gnaA* in antibiotic resistance and virulence in *Acinetobacter baumannii*. *Antimicrob Agents Chemother.* 2019 Oct;63(10):e00694-19.
- [28] Liu H, Begik O, Lucas MC, et al. Accurate detection of m(6)A RNA modifications in native RNA sequences. *Nat Commun.* 2019 Sep 9;10(1):4079.
- [29] Liu J, Yue Y, Han D, et al. A METTL3-METTL14 complex mediates mammalian nuclear RNA N6-adenosine methylation. *Nat Chem Biol.* 2014 Feb;10(2):93–95.
- [30] Jia G, Fu Y, Zhao X, et al. N6-methyladenosine in nuclear RNA is a major substrate of the obesity-associated FTO. *Nat Chem Biol.* 2011 Oct 16;7(12):885–887.
- [31] Li W, Li L, Zhang C, et al. Investigations into the antibacterial mechanism of action of Viridicatumtoxins. *ACS Infect Dis.* 2020 Jul 10;6(7):1759–1769.
- [32] San Millan A. Evolution of plasmid-mediated antibiotic resistance in the clinical context. *Trends Microbiol.* 2018 Dec;26(12):978–985.
- [33] Hua X, Liu L, Fang Y, et al. Colistin resistance in *Acinetobacter baumannii* MDR-ZJ06 revealed by a multiomics approach. *Front Cell Infect Microbiol.* 2017;7(45). doi:10.3389/fcimb.2017.00045
- [34] Sokurenko EV, Hasty DL, Dykhuizen DE. Pathoadaptive mutations: gene loss and variation in bacterial pathogens. *Trends Microbiol.* 1999 May;7(5):191–195.
- [35] Miskinyte M, Sousa A, Ramiro RS, et al. The genetic basis of *Escherichia coli* pathoadaptation to macrophages. *PLoS Pathog.* 2013;9(12):e1003802.
- [36] Yu H, Hanes M, Chrisp CE, et al. Microbial pathogenesis in cystic fibrosis: pulmonary clearance of mucoid *Pseudomonas aeruginosa* and inflammation in a mouse model of repeated respiratory challenge. *Infect Immun.* 1998 Jan;66(1):280–288.
- [37] Grana-Miraglia L, Lozano LF, Velazquez C, et al. Rapid gene turnover as a significant source of genetic variation in a recently seeded population of a health-care-associated pathogen. *Front Microbiol.* 2017;8:1817.
- [38] Sarantis H, Grinstein S. Subversion of phagocytosis for pathogen survival. *Cell Host Microbe.* 2012 Oct 18;12(4):419–431.
- [39] Hua X, Zhou Z, Yang Q, et al. Evolution of *Acinetobacter baumannii* in vivo: international clone II, more resistance to ceftazidime, mutation in *ptk*. *Front Microbiol.* 2017;8:1256.
- [40] Geisinger E, Isberg RR. Antibiotic modulation of capsular exopolysaccharide and virulence in *Acinetobacter baumannii*. *PLoS Pathog.* 2015 Feb;11(2):e1004691.
- [41] Russo TA, Luke NR, Beanan JM, et al. The K1 capsular polysaccharide of *Acinetobacter baumannii* strain 307-0294 is a major virulence factor. *Infect Immun.* 2010 Sep;78(9):3993–4000.
- [42] Okamoto S, Tamaru A, Nakajima C, et al. Loss of a conserved 7-methylguanosine modification in 16S rRNA confers low-level streptomycin resistance in bacteria. *Mol Microbiol.* 2007 Feb;63(4):1096–1106.
- [43] Nishimura K, Hosaka T, Tokuyama S, et al. Mutations in *rsmG*, encoding a 16S rRNA methyltransferase, result in low-level streptomycin resistance and antibiotic overproduction in *Streptomyces coelicolor* A3 (2). *J Bacteriol.* 2007 May;189(10):3876–3883.

- [44] Powers T, Noller HF. A functional pseudoknot in 16S ribosomal RNA. *EMBO J.* **1991 Aug**;10(8):2203–2214.
- [45] Wong SY, Javid B, Addepalli B, et al. Functional role of methylation of G518 of the 16S rRNA 530 loop by GidB in *Mycobacterium tuberculosis*. *Antimicrob Agents Chemother.* **2013 Dec**;57(12):6311–6318.
- [46] Benitez-Paez A, Villarroya M, Armengod ME. Regulation of expression and catalytic activity of *Escherichia coli* RsmG methyltransferase. *RNA.* **2012 Apr**;18(4):795–806.
- [47] Liroy VS, Goussard S, Guerineau V, et al. Aminoglycoside resistance 16S rRNA methyltransferases block endogenous methylation, affect translation efficiency and fitness of the host. *RNA.* **2014 Mar**;20(3):382–391.
- [48] Grenga L, Little RH, Chandra G, et al. Control of mRNA translation by dynamic ribosome modification. *PLoS Genet.* **2020 Jun**;16(6):e1008837.
- [49] Zhu M, Dai X. Bacterial stress defense: the crucial role of ribosome speed. *Cellular and Molecular Life Sciences: CMLS.* **2020 Mar**;77(5):853–858.
- [50] Dai X, Zhu M, Warren M, et al. Slowdown of translational elongation in *Escherichia coli* under hyperosmotic stress. *mBio.* **2018 Feb 13**;9(1):e02375-17.
- [51] Imlay JA. The molecular mechanisms and physiological consequences of oxidative stress: lessons from a model bacterium. *Nat Rev Microbiol.* **2013 Jul**;11(7):443–454.
- [52] Duggal Y, Fontaine BM, Dailey DM, et al. RNase I modulates *Escherichia coli* motility, metabolism, and resistance. *ACS Chem Biol.* **2020 Jul 17**;15(7):1996–2004.
- [53] Bechhofer DH, Deutscher MP. Bacterial ribonucleases and their roles in RNA metabolism. *Crit Rev Biochem Mol Biol.* **2019 Jun**;54(3):242–300.
- [54] Simner PJ, Patel R. Cefiderocol antimicrobial susceptibility testing considerations: the Achilles' heel of the Trojan horse? *J Clin Microbiol.* **2020 Dec 17**;59(1):e00951-20.
- [55] McCreary EK, Heil EL, Tamma PD. New perspectives on antimicrobial agents: cefiderocol. *Antimicrob Agents Chemother.* **2021 Jul 16**;65(8):e0217120.